J Appl Electrochem (2008) 38:1415–1419
DOI 10.1007/s10800-008-9581-8

ORIGINAL PAPER

Pd–Ru/C as the electrocatalyst for hydrogen peroxide reduction

Limei Sun · Dianxue Cao · Guiling Wang

Received: 15 January 2008 / Accepted: 25 April 2008 / Published online: 14 May 2008

Abstract Pd–Ru, Pd and Ru nanoparticles supported on Vulcan XC-72 carbon were prepared by chemical reduction of $PdCl_2$ and/or $RuCl_3$ in aqueous solution using $NaBH_4$ as the reducing agent. Transmission electron microscopy measurements showed that Pd–Ru particles were uniformly dispersed on carbon. The particle size of Pd–Ru is around 5–9 nm. X-ray diffraction analysis indicated that Ru formed alloy with Pd in Pd–Ru/C catalyst. The electroreduction of hydrogen peroxide on Pd–Ru/C, Pd/C and Ru/C in H_2SO_4 solution was examined by linear sweep voltammetry and chronoamperometry measurements. Results revealed that Pd–Ru/C catalyst exhibited higher electrocatalytic activity for hydrogen peroxide reduction than Pd/C and Ru/C. All the catalysts showed good stability for hydrogen peroxide electroreduction in H_2SO_4 electrolyte.

Keywords Palladium · Ruthenium · Hydrogen peroxide reduction · Electrocatalyst · Fuel cell

1 Introduction

Oxygen from air is generally used as oxidant in conventional fuel cells for terrestrial applications. However, when a fuel cell operates in special environments where air is unavailable (e.g. underwater or space), it needs liquid oxygen or compressed oxygen as oxidant. The use of these types of oxidants presents severe safety risks and increases the complexity of a fuel cell system. Hydrogen peroxide is an attractive choice in replace of compressed or liquid oxygen as oxidant for those fuel cells working in environments without air. This is because: (1) the electroreduction of hydrogen peroxide is a two-electron transfer process and hence has lower activation energy than oxygen electroreduction (4-electron reaction); (2) hydrogen peroxide is liquid at standard conditions and much denser than a gas phase oxidant, its handling, storage and feeding to a fuel cell are easy. Recently, hydrogen peroxide has been used in metal–hydrogen peroxide semi fuel cell [1–6], direct methanol–hydrogen peroxide fuel cell [7] and direct borohydride–hydrogen peroxide fuel cell [8–11].

The electrochemical reduction rate of hydrogen peroxide is a major factor determining the performance of fuel cells. Therefore, the study on electrocatalysts for H_2O_2 reduction has brought public attention in recent years in the fuel cell community. Noble metals, including Pt [12], Pd [5, 13, 14], Ir [13, 14], Au [15], Ag [5, 6, 16] and a combination of these, have been investigated as electrocatalysts for hydrogen peroxide reduction in acidic or basic medium. Among these catalysts, Pd and Pd–Ir demonstrated better overall performance in terms of high catalytic activity and low oxygen evolution activity. In this work, we prepared carbon-supported Pd–Ru catalyst and examined its catalytic activity for hydrogen peroxide electroreduction in H_2SO_4 solution, and found that Pd–Ru/C catalyst shows higher catalytic activity than Pd/C and Ru/C.

2 Experimental

2.1 Reagents

$PdCl_2$ and $RuCl_3$ were purchased from Shanxi Kaida Chemical Engineering Co., Ltd. $NaBH_4$, H_2SO_4 and H_2O_2

L. Sun · D. Cao (✉) · G. Wang
College of Material Science and Chemical Engineering,
Harbin Engineering University, Harbin 150001, P.R. China
e-mail: caodianxue@hrbeu.edu.cn

(30%) were supplied by Tianjin Hengxing Chemical Preparation Co., Ltd. Carbon black powder (Vulcan XC-72, Cabot International) with a specific surface area (BET) of 250 $m^2\ g^{-1}$ was used as the support for the catalysts. All chemicals are analytical grade and were used as-received without further purification. Ultrapure water (Millipore, 18 MΩ cm) was used throughout the study.

2.2 Catalyst preparation

Vulcan XC-72 carbon black (50 mg) was pretreated by dispersing in 65% HNO_3 solution and heating at 60 °C for 4 h. Appropriate amounts of $PdCl_2$ and $RuCl_3$ were dissolved in 10 mL ultrapure water, and 1 mol L^{-1} NaOH solution was added to adjust the pH to 7–8. The treated carbon was then dispersed into the above solution by sonication. The 10 mL $NaBH_4$ solution was added dropwise to the carbon suspension under vigorous stirring condition at room temperature. The mixture was stirred for another 2 h to allow the reaction to be completed. The solid particles were separated from the solution by filtration and washed with water thoroughly. The obtained catalysts were dried in a vacuum oven at 60 °C overnight. Pd/C and Ru/C catalysts were also obtained using the same procedure for comparison. All samples contain a total metal loading of 20 wt.%.

2.3 Catalyst characterizations

X-ray powder diffraction (XRD) patterns of the catalysts were recorded with a Rigaku D/Max-3B diffractometer (Shimadzu) using Cu Kα radiation ($\lambda = 1.5406$ Å). The 2θ angle was scanned from 10° to 90°. The Pd–Ru composition was estimated by an EDS analyzer attached to a JSM-6480 scanning electron microscope (SEM). Information on shape and size distribution was obtained with a JEOL JEM2010 transmission electron microscope (TEM).

2.4 Electrochemical measurements

Electrochemical measurements were carried out in a standard three-electrode electrochemical cell with saturated Ag/AgCl electrode as the reference and glassy carbon rod behind a D-porosity glass frit as the counter electrode. The working electrode was prepared as follows: 5 mg of the catalyst was suspended in 1 mL ultrapure water by sonicating for about 30 min to obtain the catalyst ink, 4 μL of the ink was spread on the surface of a gold disc electrode(d = 3 mm, Autolab) with a micropipette and dried in atmosphere. The resulting loading of the metal catalyst on Au disc is around 0.143 μg cm^{-2}. Cyclic volatmmetry (CV) was conducted in a 0.1 mol L^{-1} H_2SO_4 solution. Linear sweep voltammetry (LSV) and chronoamperometry (CP) were performed in 0.1 mol L^{-1} H_2SO_4 containing 0.03 mol L^{-1} H_2O_2. The 0.1 mol L^{-1} H_2SO_4 electrolyte solution was deaerated by bubbling ultra-high-purity nitrogen for 20 min before each experiment. The potential scan rate for all tests is 5 mV s^{-1} and the temperature is 20 ± 0.05 °C controlled by a thermostatic bath. Electrochemical measurements were performed using a computer-controlled potentiostat (Eco Chemie, Autolab PGSTAT302 with GPES software). All potentials in this work were referred to the normal hydrogen electrode (NHE).

3 Results and discussion

3.1 Catalyst characterizations

Figure 1 shows the TEM image of the Pd–Ru/C catalyst. It can be seen that metal particles were relatively uniformly dispersed on the surface of Vulcan XC-72. The particles have irregular shapes and the diameter of the majority of the particles is between 5 and 9 nm. A few agglomerations were observed, which may result from the fast reduction process of $NaBH_4$ [17]. Figure 2 shows the EDS spectrum of the Pd–Ru/C catalyst. The atomic ratio of Pd to Ru obtained by EDS analysis is around 1.33:1, which is slightly higher than that in the precursor. This is probably because some Ru^{3+} ions failed to be reduced simultaneously with Pd^{2+} ions, as the redox potential of Ru^{3+}/Ru($E^0 = 0.62$ V) is much lower than that of Pd^{2+}/Pd ($E^0 = 0.951$ V) [18]. Oxygen species were detected in the

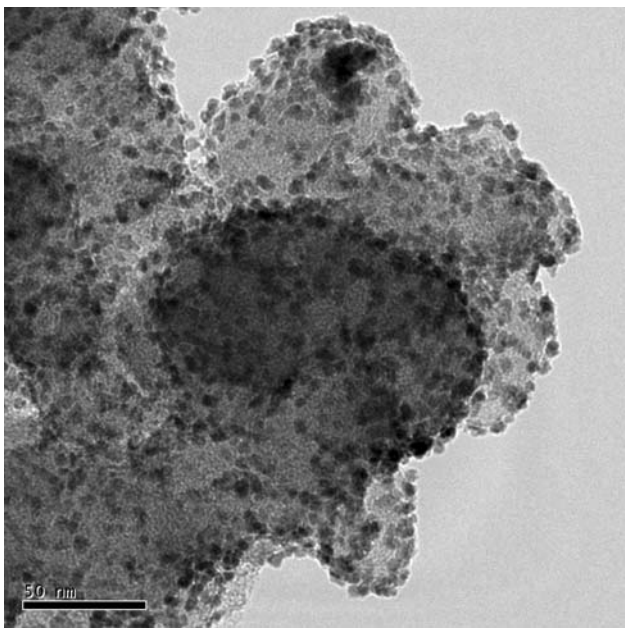

Fig. 1 TEM image of Pd–Ru/C catalyst

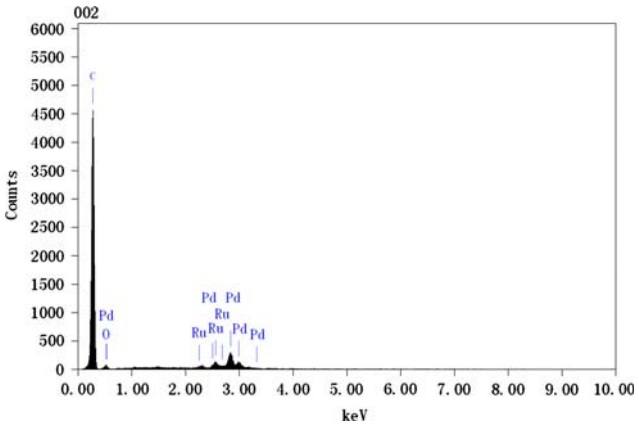

Fig. 2 EDS spectrum of Pd–Ru/C catalyst

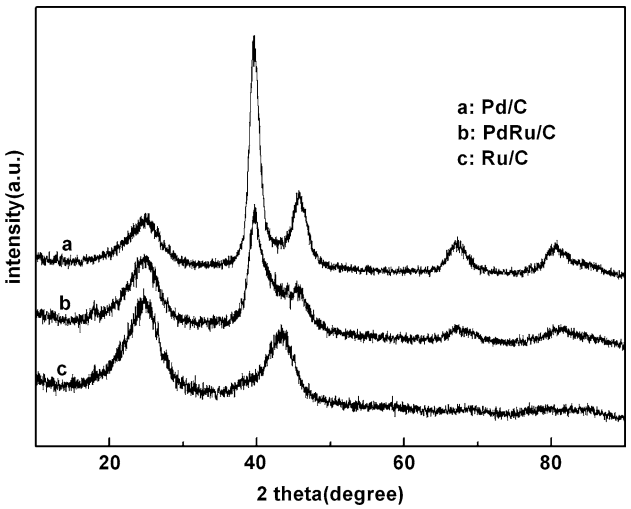

Fig. 3 XRD patterns of Pd–Ru/C, Pd/C and Ru/C catalysts

Pd–Ru/C catalyst, which is likely from the carbon support or Ru surface oxides.

Figure 3 gives the XRD patterns of Pd–Ru/C, Pd/C and Ru/C catalysts. The peak located at about 25.5° is associated with the carbon support. Diffraction peaks of Pd/C at 2θ value of 39.587°, 45.868°, 67.190°, 80.661° and 85.950° are indexed to the (111), (200), (220), (311) and (222) crystal planes, respectively. These peaks indicated that Pd/C catalyst has a face-centered cubic (fcc) structure. The pattern of Ru/C catalyst suggested the presence of hexagonal crystalline ruthenium phase. Peaks at 2θ value of 43.112° is from the (002) crystal plane. The Pd–Ru/C catalyst displayed a much similar diffraction pattern with Pd/C, except the shift of 2θ to slightly higher values and the increase of peak widths. The shift of diffraction angles is an indication of a decrease in the lattice constant, which is probably caused by the alloying of Ru with Pd because the atomic radius of Ru (1.34 Å) is smaller than that of Pd (1.38 Å) [19]. The increase of peak width suggested that the particle size of Pd–Ru/C is smaller than that of Pd/C. No peaks corresponding to metallic ruthenium or ruthenium oxides were observed, demonstrating the absence of crystal metallic Ru and Ru oxides/hydroxides in the Pd–Ru/C catalyst. However, metal Ru and its oxides may exist in amorphous phases.

3.2 Electrochemical measurements

The cyclic voltammograms of Pd–Ru/C, Pd/C and Ru/C catalysts at sweep rate of 5 mV s^{-1} in 0.1 mol L^{-1} H_2SO_4 solution are shown in Fig. 4. The upper limit potential for the positive going scan was set to be 0.8 V in order to prevent possible Ru dissolution [19, 20]. It can be clearly seen that the Pd/C catalyst displayed the main characteristics of polycrystalline Pd in acid solution [21], Two pairs of anodic and cathodic peaks observed in the potential region of 0–300 mV were hydrogen adsorption and desorption. The CV of Ru/C did not show the hydrogen region clearly due to the overlap of Ru redox potential with hydrogen adsorption/desorption potential. The CV profile of Pd–Ru/C exhibited a combination feature of Pd/C and Ru/C, i.e. the hydrogen adsorption/desorption region (0.0–0.2 V) on Pd–Ru/C is clearer than that on Ru/C, and the double layer charging currents on Pd–Ru/C in the potential region of 0.2–0.6 V are much higher than those on Pd/C. Besides, the onset potential corresponding to surface oxidation of Pd–Ru/C and Ru/C are both at around 0.25 V, which is much lower than that for the adsorption of O or OH species on Pd/C (around 0.7 V). All these observations suggested the presence of Ru on the surface of Pd–Ru/C catalyst.

Figure 5 shows linear sweep voltammograms of Pd–Ru/C, Pd/C and Ru/C catalysts measured at 500 rpm rotation

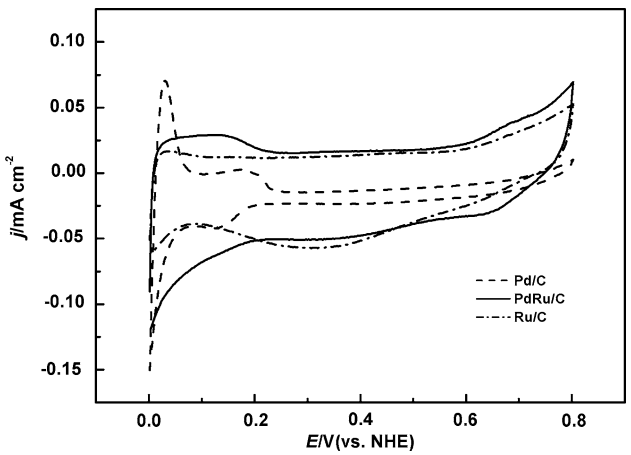

Fig. 4 Cyclic voltammograms of Pd–Ru/C, Pd/C and Ru/C catalysts recorded in 0.1 mol L^{-1} H_2SO_4 solution at 5 mV s^{-1}

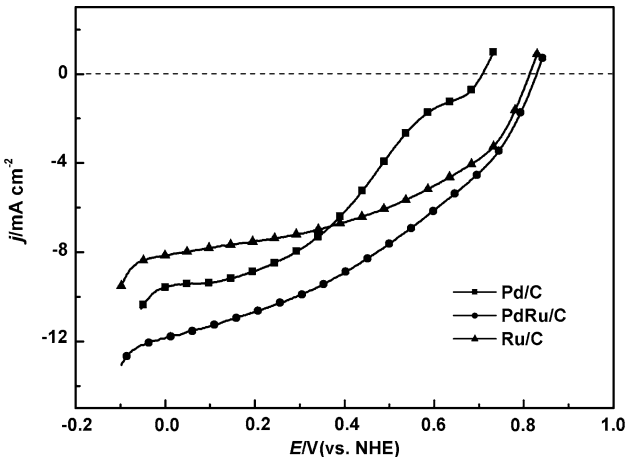

Fig. 5 The current–potential curves of H_2O_2 electroreduction on different catalysts in 0.1 mol L^{-1} H_2SO_4 + 0.03 mol L^{-1} H_2O_2. Scan rate: 5 mV s^{-1}, Rotation rate: 500 rpm

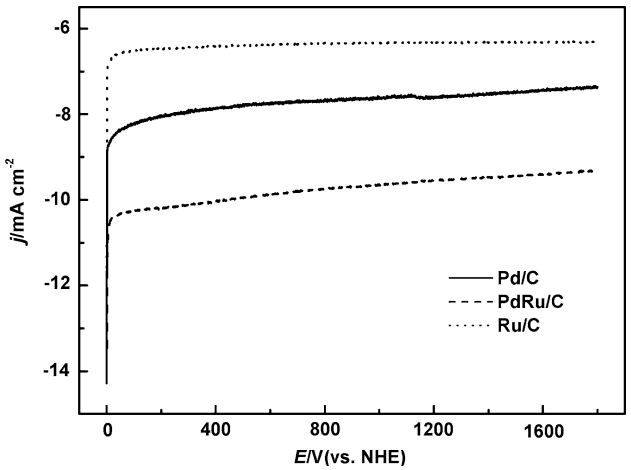

Fig. 6 Current–time curves of H_2O_2 electroreduction on different catalysts in 0.1 mol L^{-1} H_2SO_4 + 0.03 mol L^{-1} H_2O_2. $E = 0.0$ V, Scan rate: 5 mV s^{-1}, Rotation rate: 500 rpm

rate in 0.1 mol L^{-1} H_2SO_4 containing 0.03 mol L^{-1} H_2O_2. It can be seen that all the three catalysts exhibited catalytic activities for hydrogen peroxide electroreduction in acid electrolyte. However, Pd/C displayed a lower onset potential but a larger limiting current density for hydrogen peroxide reduction than Ru/C. The Pd–Ru/C catalyst showed superior catalytic activity for hydrogen peroxide reduction than both Pd/C and Ru/C. The onset potential of H_2O_2 reduction on Pd–Ru/C is similar to that on Ru/C (around 0.8 V), but about 0.1 V more positive than that on Pd/C. The current densities for hydrogen peroxide electroreduction on Pd–Ru/C catalyst are higher than that on Pd/C and Ru/C catalysts within the whole potential range tested. This high activity of Pd–Ru/C catalyst demonstrated the promotion effect of Ru to Pd for hydrogen peroxide electroreduction. The onset potential for hydrogen peroxide electroreduction is close to that for oxygen reduction on Pt [22]. Therefore, Pd–Ru/C catalyst is a promising effective cathode catalyst for fuel cells using H_2O_2 as oxidant.

In order to further compare the electrocatalytic performance of Pd–Ru/C, Pd/C and Ru/C towards the hydrogen peroxide electroreduction, chronoamperometry tests were conducted in 0.1 mol L^{-1} H_2SO_4 + 0.03 mol L^{-1} H_2O_2 at the constant potential of 0.0 V. The results are given in Fig. 6. After a rapid initial decrease, the current density reached steady-state. The steady-state current density for Ru/C nearly remained unchanged within 30 min. However current density for Pd–Ru/C and Pd/C slightly decreased with time elongation. The final current densities after holding the potential at 0.0 V for 30 min were 9.5 mA cm^{-2} for Pd–Ru/C, 7.5 mA cm^{-2} for Pd/C and 6.5 mA cm^{-2} for Ru/C. Clearly, Pd–Ru/C catalyst showed higher catalytic activity for hydrogen peroxide electroreduction than Pd/C and Ru/C.

4 Conclusions

Vulcan XC-72 supported Pd–Ru, Pd and Ru catalysts were prepared by the chemical reduction of metal precursors using sodium borohydride as the reductant at room temperature. Pd–Ru nanoparticles were dispersed uniformly on the carbon support and have particle size of around 5–9 nm. Ru formed alloys with Pd as indicated by XRD analysis. Pd–Ru/C catalyst displayed much higher activity for hydrogen peroxide electroreduction than Pd/C and Ru/C catalysts, demonstrating the promotion function of Ru to Pd. Pd–Ru/C catalyst is a promising cathode catalyst for fuel cells using H_2O_2 as oxidant.

Acknowledgements This work was financially supported by Harbin Engineering University through the foundation for the innovation platform of underwater power source (HEUFT07030).

References

1. Hasvold Ø, Johansen KH (1999) J Power Sources 80:254
2. Marsh CL, Licht SL, Matthews DE (1995) U. S. Patent, 5445905
3. Dow EG, Yan SG, Medeiros MG et al (2003) U. S. Patent, 0124418
4. Medeiros MG, Bessette RR (2004) J Power Sources 136:226
5. Yang W, Yang S, Sun W et al (2006) Electrochim Acta 52:9
6. Yang W, Yang S, Sun W et al (2006) J Power Sources 160:1420
7. Prater DN, Rusek JJ (2003) Appl Energy 74:135
8. Raman RK, Prashant SK, Shukla AK (2006) J Power Sources 162:1073
9. Miley GH, Luo N, Mather J et al (2007) J Power Sources 165:509
10. Choudhury NA, Raman RK, Sampath S et al (2005) J Power Sources 143:1
11. Ponce de león C, Walsh FC, Rose A et al (2007) J Power Sources 164:441
12. Van Venrooij TGJ, Koper MTM (1995) Electrochim Acta 40:1689

13. Bessette RR, Cichon JM, Dischert DW et al (1999) J Power Sources 80:248
14. Bessette RR, Medeiros MG, Patrissi CJ et al (2001) J Power Sources 96:240
15. Štrbac S, Adžić RK (1992) J Electroanal Chem 337:355
16. Flatgen G, Wasle S, Lubke M et al (1999) Electrochim Acta 44:4499
17. Cao L, Sun G, Li H et al (2007) Electrochem Commun 9:2541
18. Guo J, Sun G, Wang Q et al (2006) Carbon 44:152
19. Li H, Sun G, Cao L et al (2007) Electrochim Acta 52:6622
20. Solla-Gullon J, Vidal-Iglesias FJ, Montiel V et al (2004) Electrochim Acta 49:5079
21. Pattabiraman R (1997) Appl Catal A Gen 153:9
22. Elezović NR, Babić BM, Radmilović VR et al (2008) J Power Sources 175:250